www.sciencemag.org/cgi/content/full/1140300/DC1

Supporting Online Material for

Functional Quantum Nodes for Entanglement Distribution over Scalable Quantum Networks

Chin-Wen Chou, Julien Laurat, Hui Deng, Kyung Soo Choi, Hugues de Riedmatten, Daniel Felinto, H. Jeff Kimble*

*To whom correspondence should be addressed. E-mail: hjkimble@caltech.edu

Published 5 April 2007 on *Science* Express
DOI: 10.1126/science.1140300

This PDF file includes:

Supporting Online Material – Functional Quantum Nodes for Entanglement Distribution over Scalable Quantum Networks

Chin-Wen Chou, Julien Laurat, Hui Deng, Kyung Soo Choi, Hugues de Riedmatten, Daniel Felinto, H. J. Kimble
Norman Bridge Laboratory of Physics 12-33, California Institute of Technology, Pasadena, California 91125, USA
(Dated: March 23, 2007)

Supporting documentation is provided for our manuscript Ref. [1].

I. EXPERIMENTAL DETAILS

Ensembles (LU, LD) are pencil-shaped groups of cold Cesium atoms in a magneto-optical trap (MOT) while ensembles (RU, RD) are in another MOT, 3 meters away. $\{|g\rangle, |s\rangle, |e\rangle\}$ correspond to the hyperfine levels $\{|6S_{1/2}, F = 4\rangle, |6S_{1/2}, F = 3\rangle, |6P_{3/2}, F' = 4\rangle\}$, respectively. In each MOT, the ensembles U, D are separated by 1 mm by way of birefringent beam displacers [2]. The MOT is formed at a repetition rate of 40 Hz. In each cycle, the MOT is loaded for 18 ms, after which the magnetic field is quickly switched off. The trapping beams are turned off 3 ms after the magnetic field, while the repumping beam stays on for another 100 μs before being switched off in order to prepare the atoms in the $F = 4$ ground state $|g\rangle$. 3.4 ms after the magnetic field is turned off, trials of the protocol (each consisting of successive write, read, and repumping pulses) are repeated with 575 ns period for 3.4 ms. In each trial, the write pulse is ≈ 30 ns in duration and 10 MHz red-detuned from the $|g\rangle \rightarrow |e\rangle$ transition. The read pulse and the repumping pulse are both derived from the read beam (resonant with the $|s\rangle \rightarrow |e\rangle$ transition) with 30 ns and 75 ns duration, respectively. The read pulse is closely followed by the repumping pulse. The read pulse is delayed ≈ 400 ns after the write pulse, leaving time for the control logic to gate it off, along with the subsequent pulses. Independent phase stability measurements show that the phase η drifts in a negligible way, $(\pi/30)$ over $500\mu s$ corresponding to 870 trials. Some other parameters of the experiments are calibrated and listed in the table I below:

TABLE I: Noise and Efficiencies

	U	D
Field 1 dark count rate	~ 10 Hz	~ 10 Hz
Field 2 dark count rate	~ 100 Hz	~ 100 Hz
Overall retrieval efficiency p_c	$6.4\% \pm 0.5\%$	$8.0\% \pm 0.5\%$
Field 2 propagation loss	$68 \pm 5\%$	$68 \pm 5\%$
Field 2 photon detection efficiency	$50 \pm 5\%$	$50 \pm 5\%$

II. FRINGE VISIBILITY AS A FUNCTION OF $h^{(2)}$

Let us consider that the two pairs of ensembles, U and D, have been prepared by heralded detections at D_{1a}, D_{1b} and D_{1c}, D_{1d}. Denote by p_{10}, p_{01}, and p_{11} the probability p_{ij} to register i photodetection events in field 2_{LU} and j in field 2_{RU} after firing the read pulses. We will assume, for simplicity, the various p_{ij} are the same for both pairs of ensembles. For each of them, the suppression of the two-photon events relative to the square of the probability for single-photon events is characterized by the parameter $h^{(2)}$[3]:

$$h^{(2)} = \frac{p_{11}}{p_{10}p_{01}}\,. \tag{1}$$

We next relate $h^{(2)}$ to the maximal C_{max} and minimal C_{min} coincidence probabilities between various output ports of the detection polarizing beamsplitters (PBS) for the left and right nodes at detectors D_{2a}, D_{2b} and D_{2c}, D_{2d} (see Fig. 1 of Ref. [1]). Consider, for example, the transmitted ports of the PBS at the L, R detectors for the case that the left node has the half-wave plate $(\frac{\lambda}{2})_L$ set to 0°. In this case, fields 2_{LU} and 2_{LD} are detected independently, with field 2_{LD} transmitted at the PBS. On one hand, C_{max} is obtained for crossed polarizers (i.e., $(\frac{\lambda}{2})_R$ set to 45° at the right node, with then field 2_{RU} transmitted) and is given to lowest order by:

$$C_{max} = p_{10}p_{01}. \tag{2}$$

This term corresponds to the case where only a single excitation is distributed in each pair, and each retrieved photon is detected from a transmitted port on each side L, R.

On the other hand, the minimum coincidence probability C_{min} is obtained for parallel polarizers (i.e., $(\frac{\lambda}{2})_R = 0°$ at the right node, with then field 2_{RD} transmitted) and can be written as:

$$C_{min} = p_{11}. \tag{3}$$

This term corresponds to coincidences due to photons coming from the same pair of ensembles. The smaller is the excitation probability, the smaller is this background term.

Taking Eqs. (2) and (3) into account, we find that the visibility for the number of coincidences as a function of the right polarizer angle (i.e., the angle for $(\frac{\lambda}{2})_R$) is given by:

$$V = \frac{C_{max} - C_{min}}{C_{max} + C_{min}} = \frac{1 - h^{(2)}}{1 + h^{(2)}} \ . \tag{4}$$

Assuming that the visibility is the same in each basis, we then find a CHSH parameter S equal to [4]:

$$S = 2\sqrt{2}\, V = 2\sqrt{2}\, \frac{1 - h^{(2)}}{1 + h^{(2)}} \ . \tag{5}$$

A minimal value $h^{(2)}_{min} = 0.17$ is thus required to violate the CHSH inequality $S < 2$ in the absence of any imperfections except the intrinsic two-photon component. This value underlines that this experiment is much more stringent in terms of minimization of high-order terms than previously reported setups. For example, in Ref. [5], where entanglement between a photon and a stored excitation is reported, a value of $h^{(2)}$ equal to 0.68 was sufficient to violate the inequality. The dramatic improvement reported recently by different groups for the quality of the photon pairs emitted by an atomic ensemble was thus an enabling step for the practical realization of such a more elaborate procedure involving a total of 4 ensembles reported in Ref. [1].

III. TWO-PHOTON INTERFERENCE AND INFERRED OVERLAPS

For a non-perfect overlap ξ of the field-2 photon wavepackets, the visibility of the fringes in the 45° basis is decreased by a factor ξ^2. This overlap can be determined by two-photon interference, which is implemented by mixing the fields 2_U and 2_D on each side (Right and Left) by rotating the half-wave plates $(\frac{\lambda}{2})_L, (\frac{\lambda}{2})_R$ by 22.5°. If the single photon wavepackets are indistinguishable, no coincidences should be observed. However, the two-photon component can lead to coincidences, which reduce the visibility. Let us determine the expected visibility as a function of the two-photon component by way of a simple model.

Consider P_n the probability of finding n photons in field 2, and assume the various P_n are the same for both ensembles involved. In the ideal case where all ensembles have the same properties, the two-photon suppression for each field 2 can also be characterized by the same $h^{(2)}$ parameter used before, which can be written here as:

$$h^{(2)} = \frac{2P_2}{P_1^2}. \tag{6}$$

When the half-wave plates $(\frac{\lambda}{2})_L, (\frac{\lambda}{2})_R$ are at 0°, the fields 2 are detected independently and the probability p_{max} to register coincidences is given by:

$$p_{max} = P_1^2. \tag{7}$$

When the half-wave plates $(\frac{\lambda}{2})_L, (\frac{\lambda}{2})_R$ are rotated to 22.5°, if the two fields overlap perfectly, the term with one photon in each input does not lead to coincidences. If we denote by ξ the overlap, the probability p_{min} to have one photon in each output is then:

$$p_{min} = \frac{(1 - \xi^2)}{2} P_1^2 + \frac{P_2}{2} + \frac{P_2}{2} = [1 - \xi^2 + h^{(2)}] \frac{P_1^2}{2} \ . \tag{8}$$

From these two probabilities, we find that the visibility of the dip in coincidences can be written as:

$$V_{dip} = \frac{p_{max} - p_{min}}{p_{max}} = \frac{1 + \xi^2 - h^{(2)}}{2}. \tag{9}$$

In our case, the measured visibility V_{dip} is $85 \pm 2\%$ for the left node and $89 \pm 2\%$ for the right one. The measured average $h^{(2)}$ parameter for this set of data is 0.09 ± 0.01, which should lead in the case of perfect overlap to visibilities $V_{\rm model} = 95.5 \pm 0.5\%$. From the measured visibilities and this simple model, we can then estimate the overlaps: $\xi = 0.89 \pm 0.03$ for the left node and $\xi = 0.93 \pm 0.03$ for the right node.

IV. DECOHERENCE TIME OF THE STORED EXCITATION

Residual magnetic fields, which lead to inhomogeneous broadening of the ground states levels, is the major limiting factor of the coherence time τ_c of the stored excitation [5, 7]. Consequently, if we neglect dark counts, the conditional retrieval efficiency $p_c = p_{01} + p_{10}$ is expected to decay exponentially with the storage time τ_M:

$$p_c = p_c^0 \exp(-\frac{\tau_M}{\tau_c}). \tag{10}$$

Figure 1 shows an independent measurement of p_c vs. τ_M, with the U and D pairs separated. Fitting the data with Eq. 10 gives, for the U and D pairs respectively, $p_c^0 = 7.0\% \pm 0.1\%$ and $8.7\% \pm 0.2\%$, and $\tau_c = 9.1 \pm 0.6$ μs and 8.5 ± 0.5 μs.

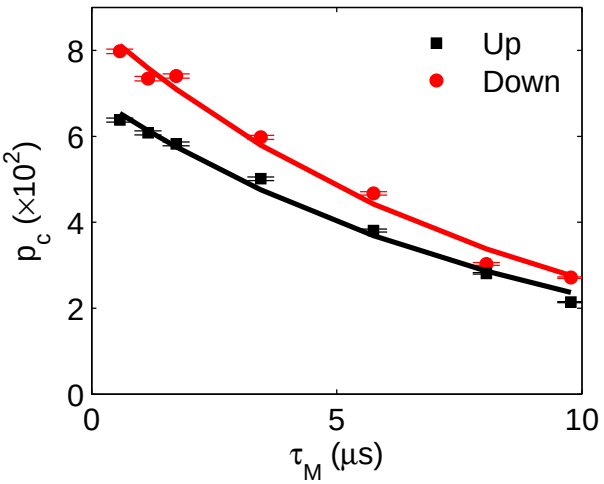

FIG. 1: Conditional probability p_c of detecting one photon in a field 2 for the U (black squares) and D (red circles) pairs, as a function of the storage time τ_M of an excitation. The error bars indicate statistical errors. The solid lines are fits using Eq. 10.

The decay of p_c leads to a similar exponential decay of C_{ij}. C_{ij} $(i, j = a, b, c, d)$ are the coincidence count rates of two field 2 photons conditioned on two heralding field 1 photons defined before. Summing over all C_{ij} used in calculating $S_\pm$, we obtain the total coincidence count rates $C_{S\pm}$ for the measurement of the Bell parameters S_+ and S_-. $C_{S\pm}(\tau_M)$ corresponds to the probability distribution of the $S_\pm(\tau_M)$, and is reflected in the statistical error bars $\Delta S_\pm(\tau_M)$. The decay of $C_{S\pm}$ with τ_M is shown in Fig. 2. Fitting the data with exponential functions:

$$C_{S\pm} = C_{S\pm}^0 \exp(-\tau_M/\tau_\pm), \quad \tau_M > 0, \tag{11}$$

gives $\tau_+ = 9.1 \pm 0.4$ μs and $\tau_- = 8.1 \pm 0.3$ μs, in good agreement with τ_c. Note that $C_{S\pm}^0 = 2C_{S\pm}(\tau_M = 0)$, since $C_{S\pm}(\tau = 0)$ is conditioned on two excitation in a same trial, while $C_{S\pm}(\tau > 0)$ is conditioned on two excitations created in two different trials: the factor of two accounts for the two possible orders of excitations ('U' then 'D' or 'D' then 'U').

V. CONDITIONAL CONTROL AND INCREASE IN GENERATION RATE

As demonstrated in Ref. [6], the conditional control of remote memories enables a large enhancement of coincidence rates relative to the case where no logic is implemented. If the state prepared in one pair of ensembles is held up to N trials, the rate for preparing both pairs is increased by a factor $(2N + 1)$ for very low excitation probability [6]. Figure 3(a) gives the probability p_{11} of simultaneously preparing the two pairs. After 17 trials, an increase by a factor 34 is obtained experimentally, close to the expected value of 35. The gain in the probability p_{1122} of generating the effective entangled state is expected to be the same if the coherence time is long enough. However, our finite coherence time results in a smaller increase of the probability to detect field 2 coincidences. This increase is given in Fig. 3(b), with a comparison to the ideal case of very long coherence time. A 19-fold enhancement is finally obtained. Let us note that the different experimental rates can be obtained from these probabilities times the number of trials per second ($\sim 2.36 \times 10^5$/s).

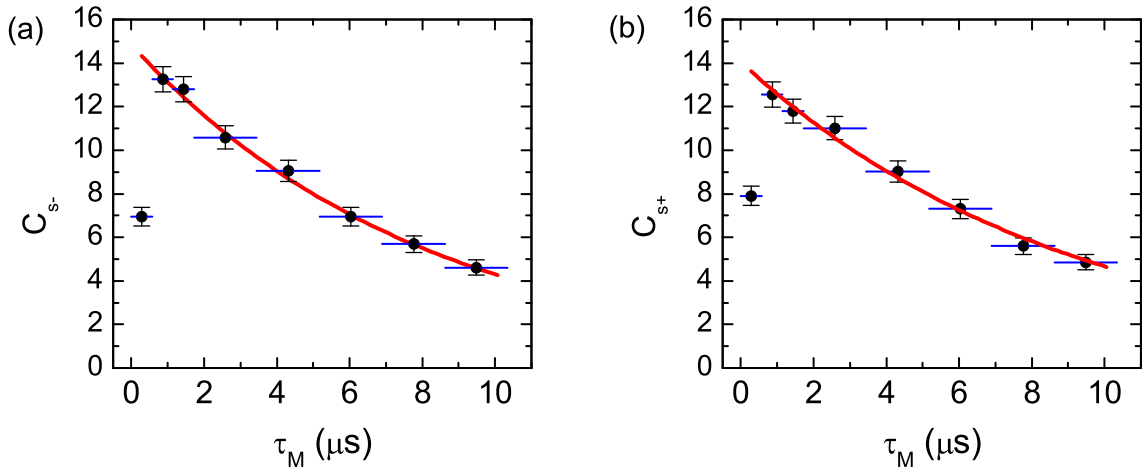

FIG. 2: The τ_M dependence of the total conditional count rates $C_{S\pm}$ in the measurement of (a) S_+ and (b) S_-. The horizontal thick lines indicate the size of the memory bin. The error bars indicate statistical errors. The solid lines are fits using Eq. 11.

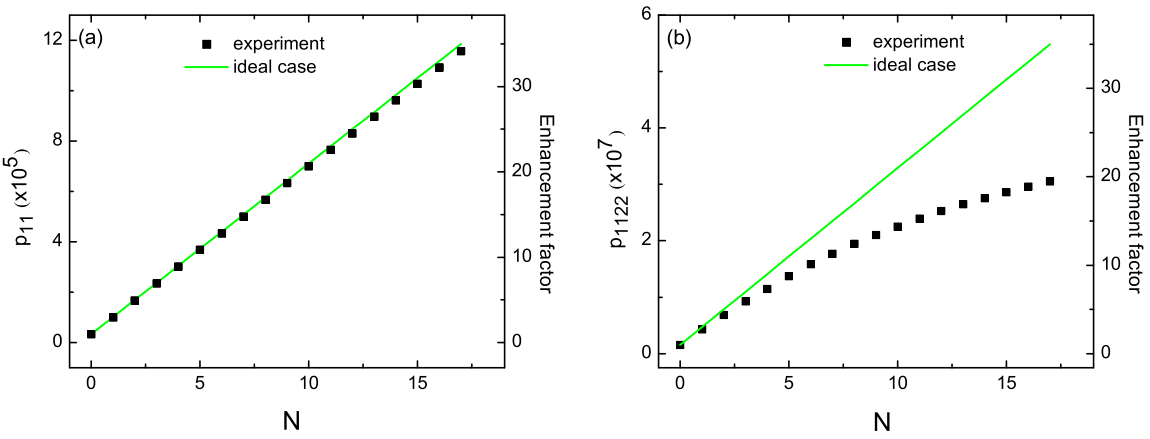

FIG. 3: Probabilities of coincidence detection as functions of the number of trials N for which the first prepared pair holds the state. (a): measured probability p_{11} of preparing the two pairs. (b): measured probability p_{1122} of detecting field 2 coincidences. The green solid line corresponds to the ideal case of very long coherence time. Both panels give in addition to these probabilities the enhancement factor obtained relative to the case without conditional control.

VI. CORRELATION FUNCTIONS $E(0°, \theta_R)$, $E(45°, \theta_R)$ FOR THE IDEAL EFFECTIVE STATE

In practice, various imperfections lead to deviations from the ideal effective state, Eq. (2) in Ref. [1]. We have developed a detailed model relevant to our experiment, but consider here only a generic form. Collective excitations are not shared with equal amplitudes between a pair of ensembles because of nonidealities in the writing and heralding processes. Likewise, the mapping of atomic states to states of field 2 by the read pulses is not ideal. Overall, these

various imperfections lead to a state $|\psi_{2_{LU},2_{RU},2_{LD},2_{RD}}\rangle$ for field 2 given by (neglecting multi-photon processes):

$$\begin{aligned}|\psi_{2_{LU},2_{RU},2_{LD},2_{RD}}\rangle &= \Big(\epsilon_{RU}|0_{2_{LU}}\rangle|1_{2_{RU}}\rangle \pm e^{i\eta_U}\epsilon_{LU}|1_{2_{LU}}\rangle|0_{2_{RU}}\rangle\Big) \\ &\otimes\Big(\epsilon_{RD}|0_{2_{LD}}\rangle|1_{2_{RD}}\rangle \pm e^{i\eta_D}\epsilon_{LD}|1_{2_{LD}}\rangle|0_{2_{RD}}\rangle\Big) \\ &= \epsilon_{RU}\epsilon_{RD}|0_{2_{LU}}\rangle|0_{2_{LD}}\rangle|1_{2_{RU}}\rangle|1_{2_{RD}}\rangle \pm e^{i\eta_U}e^{i\eta_D}\epsilon_{LU}\epsilon_{LD}|1_{2_{LU}}\rangle|1_{2_{LD}}\rangle|0_{2_{RU}}\rangle|0_{2_{RD}}\rangle \\ &\pm e^{i\eta_U}\epsilon_{RD}\epsilon_{LU}|1_{2_{LU}}\rangle|0_{2_{LD}}\rangle|0_{2_{RU}}\rangle|1_{2_{RD}}\rangle \pm e^{i\eta_D}\epsilon_{RU}\epsilon_{LD}|0_{2_{LU}}\rangle|1_{2_{LD}}\rangle|1_{2_{RU}}\rangle|0_{2_{RD}}\rangle\ , \end{aligned} \quad (12)$$

where ϵ_X is the probability amplitude that a photon is created in field 2_X. The first and second terms in the expansion correspond to the cases that the two excitations are both retrieved at node "right" and "left", respectively. Thus the effective state that yields one detection event at node "left" and the other at node "right" consists of the last two terms. After the fields are combined by PBS_L and PBS_R, we get the (unnormalized) effective state of fields 2_L and 2_R

$$|\psi_{2_L,2_R}\rangle_{eff} = \alpha|H_{2_L}V_{2_R}\rangle \pm \beta|V_{2_L}H_{2_R}\rangle\ , \quad (13)$$

where $\alpha \propto e^{i\eta_D}\epsilon_{RU}\epsilon_{LD}$ and $\beta \propto e^{i\eta_U}\epsilon_{RD}\epsilon_{LU}$.

From the effective state $|\psi_{2_L,2_R}\rangle_{eff}$, we can derive the various coincidence probabilities P_{ij}, $i,j \in \{a,b,c,d\}$, where $\{a,b,c,d\}$ refers to the detectors $D_{2\{a,b,c,d\}}$ for field 2 in Fig. 1 of Ref. [1]. When θ_L is fixed at 0°, we find (assuming unity detection efficiency)

$$\begin{aligned} P_{ac} &= |\alpha|^2\sin^2\theta_R \\ P_{bd} &= |\beta|^2\sin^2\theta_R \\ P_{ad} &= |\alpha|^2\cos^2\theta_R \\ P_{bc} &= |\beta|^2\cos^2\theta_R \\ E(0^\circ,\theta_R) &\propto P_{ac}+P_{bd}-P_{ad}-P_{bc} = -\cos(2\theta_R) \end{aligned} \quad (14)$$

irrespective of the $\pm$ sign.

By contrast, when θ_L is fixed at 45°, we obtain

$$\begin{aligned} P_{ac} &= \frac{1}{4}[1 \pm 2|\alpha||\beta|\ \cos\phi\ \cos(90^\circ - 2\theta_R) \\ &+\ (|\beta|^2 - |\alpha|^2)\ \sin(90^\circ - 2\theta_R)]\ , \end{aligned}$$

where $\phi = arg(\beta) - arg(\alpha)$. Let $\alpha = \cos\varphi$, and $\beta = \sin\varphi$. Denoting $\delta = 45^\circ - \theta_R$, we have

$$\begin{aligned} P_{ac} &= \frac{1}{4}[1 \pm |\sin2\varphi|\ \cos\phi\ \cos2\delta - \cos2\varphi\ \sin2\delta] \\ P_{bd} &= \frac{1}{4}[1 \pm |\sin2\varphi|\ \cos\phi\ \cos2\delta + \cos2\varphi\ \sin2\delta] \\ P_{ad} &= \frac{1}{4}[1 \mp |\sin2\varphi|\ \cos\phi\ \cos2\delta + \cos2\varphi\ \sin2\delta] \\ P_{bc} &= \frac{1}{4}[1 \mp |\sin2\varphi|\ \cos\phi\ \cos2\delta - \cos2\varphi\ \sin2\delta] \\ E(45^\circ,\theta_R) &\propto P_{ac}+P_{bd}-P_{ad}-P_{bc} \\ &= \pm|\sin2\varphi|\ \cos\phi\ \cos2\delta. \end{aligned} \quad (15)$$

From the expression for $E(45^\circ,\theta_R)$, we see that the deviation of $|\alpha|$ and $|\beta|$ from the balanced value, $1/\sqrt{2}$, will lead to reduction in the visibility of $E(45^\circ,\theta_R)$ fringes and thus the magnitudes of the CHSH parameters $S_{(\pm)}$. We believe that such an imbalance is responsible for the results displayed in Fig. 3(b) for $E(45^\circ,\theta_R)$ and Fig. 4 for $S_{(\pm)}$ at $\tau_M = 0$ in Ref. [1], with measurements underway to quantify this association.

Note that another combination of P_{ij}'s given above results in

$$\begin{aligned} F(45^\circ,\theta_R) &\equiv -P_{ac}+P_{bd}+P_{ad}-P_{bc} \\ &= \cos2\varphi\ \sin2\delta. \end{aligned} \quad (16)$$

$F(45°, \theta_R)$ allows us to determine φ and thus the magnitude of the coefficients α and β, independent of ϕ. Specifically, the visibility of the $F(45°, \theta_R)$ fringes normalized to that of $E(0°, \theta_R)$ fringes yields $\cos 2\varphi$.

---

[1] C.W. Chou *et al.*, manuscript submitted to *Science* (2007).

[2] C.W. Chou, PhD Thesis, Chapter 8, California Institute of Technology, May 2006, http://www.its.caltech.edu/ qoptics/thesis.html

[3] C.W. Chou *et al.*, Measurement-induced entanglement for excitation stored in remote atomic ensembles. *Nature* **438**, 828-832 (2005).

[4] I. Marcikic *et al.*, Distribution of time-bin entangled qubits over 50 km of optical fiber. *Phys. Rev. Lett.* **93**, 180502 (2004).

[5] H. de Riedmatten *et al.*, Direct measurement of decoherence for entanglement between a photon and stored atomic excitation. *Phys. Rev. Lett.* **97**, 113603 (2005).

[6] D. Felinto *et al.*, Conditional control of the quantum states of remote atomic memories for quantum networking. *Nature Physics* **2**, 844-848 (2006); advance online publication, (doi:10.1038/nphys450).

[7] D. Felinto, C.W. Chou, H. de Riedmatten, S.V. Polyakov, H.J. Kimble, Control of decoherence in the generation of photon pairs from atomic ensembles. *Phys. Rev. A* **72**, 053809 (2005).